The Impact of Nanoparticles and Aging on AC Dielectric Strength of Nomex Polymeric Composite: Weibull Distribution Based Analysis

Soumyadeep Maity
Department of Electrical Engineering, National Institute of Technology, Mizoram, India
soumya.ee95@gmail.com (corresponding author)

Sandipan Kumar Paul
Department of Electrical Engineering, Jadavpur University, Kolkata, India
sandipanpaul05@gmail.com

Biswajit Chakraborty
Department of Electrical Engineering, Jadavpur University, Kolkata, India
biswajit.chakraborty1991@gmail.com

Subhajit Maur
Department of Electrical Engineering, Ramakrishna Mahato Government Engineering College, India
subhajitmaur9153@gmail.com

Arpan Kumar Pradhan
Department of Electrical Engineering, Jadavpur University, Kolkata, India
arpan.pradhan85@gmail.com

Sovan Dalai
Department of Electrical Engineering, Jadavpur University, Kolkata, India
sovandalai@yahoo.co.in

Biswendu Chatterjee
Department of Electrical Engineering, Jadavpur University, Kolkata, India
biswenduc@gmail.com

Saibal Chatterjee
Department of Electrical Engineering, National Institute of Technology, Mizoram, India
saibalda@ieee.org

Received: 5 June 2025 | Revised: 2 July 2025 | Accepted: 7 July 2025

 DOI: https://doi.org/10.48084/etasr.12584

ABSTRACT

This research investigated the influence of insulating (Al_2O_3), semiconducting (TiO_2), and conducting (Fe_3O_4) Nanoparticles (NPs) on the breakdown strength of Nomex-based polymeric Nanocomposites (NCs). Seven samples were fabricated and thermally aged at 145 °C for 600 h to simulate accelerated degradation. Fourier Transform Infrared Spectroscopy (FTIR) was conducted to unaged, 300 h, and 600 h aging durations to examine the chemical alteration and understand the NP-induced resistance of meta-aramid polymeric chains against the thermal aging. The AC Breakdown Voltage (ACBDV) was measured every

100 h of aging, and the results were analyzed using the Weibull distribution to extract the scale parameters, shape parameters, and p-values. Cumulative breakdown probabilities at 1%, 10%, and 50% risk levels were evaluated to assess the impact of different NPs on the breakdown mechanism. After 600 h of aging, the incorporation of 1 wt% Al_2O_3 improved the BDV of pristine Nomex by 28.2%. At a 50% risk probability, BDV enhancements of 63.16% (Al_2O_3), 48.89% (TiO_2), and 42.39% (Fe_3O_4) were achieved, demonstrating the superior performance of NP-reinforced Nomex insulation under thermal stress..

Keywords-FTIR; nanocomposite; Nomex polymer; Weibull distribution; dry-type insulation

I. INTRODUCTION

Transformers play a critical role in power networks, addressing the growing demand for electricity with reliable and long-lasting performance. However, traditional liquid-filled insulation systems present notable disadvantages, including fire hazards, maintenance, and environmental concerns, such as land pollution from spilled or used oil. Except these, several cases of transformer oil ignition have resulted in huge economic losses.

To address these challenges, dry-type insulation systems with high thermal performance are gaining attention as a more efficient solution, due to non-inflammable, non-hygroscopic and cost-effective maintenance [1, 2]. Among the various dry type insulation materials, Nomex polymers -comprised of met-aramid- are widely used in electrical engineering applications, such as transformers and electrical machines. They are formed from flocs (short fibers) and fibrids (tiny binder particles). Their meta-aramid composition offers high thermal stability due to their high temperature resistant property, a reliable chemical structure, and strong intra-molecular connections. However, a declining nature in the field of mechanical and dielectric strength is observed with the prolonged exposure at higher temperatures [3].

It has been observed that the dielectric and thermal characteristics as well as the mechanical strength of dry-type insulation systems can be enhanced by the addition of several inorganic NPs, such as Al_2O_3, TiO_2, Fe_3O_4, and h-BN [4]. Particularly, authors in [5] indicated that Al_2O_3 enhanced the dielectric properties, while it also served as an effective barrier against charge bombardment, significantly reducing the risk of molecular chain rupture in polymeric insulation. In [6], TiO_2 with dry-type insulation improved the mobility of polymeric chains, which restricted the formation of deep traps at the interaction zone. Additionally, authors in [7] demonstrated that Fe_3O_4 increased the thermal property of the insulation. Based on these experiments, this study explored the above-mentioned NP for the performance of dry-type insulation systems.

To investigate the quality of insulation, the measurement of ACBDV acts as a promising parameter, mainly influenced by aging, moisture and defects, impurities, environmental conditions, and electric field stress. The Weibull distribution is a generally utilized tool to statistically analyze the ACBDV of the electrical insulation [8, 9]. It enables the engineers to identify the probability of failures at different voltage levels and is suitable for High-Voltage (HV) applications for insulation diagnostics, quality assessment, and lifetime estimation. In this study, seven types of Nomex-based NC polymeric insulation samples were developed in the laboratory, considering Al_2O_3, TiO_2, Fe_3O_4 NP at concentrations of 0.5 wt% and 1 wt%.

II. THEORETICAL BACKGROUND OF STATISTICAL ANALYSIS

To analyze the breakdown strength of the dielectric materials, a statistical analysis based on the Weibull distribution has been conducted. The Weibull plot is a graphical representation of the breakdown data of the insulting material to access the reliability and failure characteristics. The cumulative Weibull distribution function can be written as:

$$F(t) = (1 - e^{\frac{1}{\alpha}\beta}) \quad (1)$$

where t signifies the measured data of the breakdown voltages, α represents the scale parameter associated with the scattering of the measured data, and β is denoted as the shape parameter or the slope of the Weibull plot.

To determine if the measured data complied with the Weibull distribution, a hypothesis test was conducted. Specifically, the Anderson-Darling hypothesis test was used to calculate the p-value, which is defined as the probability that quantifies the strength of evidence against the null hypothesis. To determine whether the data follow a normal distribution, a vital comparison between the p-value to the significance level is required. Usually, a significance level of value α is considered [10].

The Weibull distribution was validated using a significance level of $\alpha = 0.05$. Generally, a p-value less than or equal to 0.05 indicates strong evidence against a null hypothesis, suggesting that the data do not follow a normal distribution [11, 12]. Conversely, p-values greater than 0.05 imply that the null hypothesis cannot be rejected, and the data are assumed to conform to the Weibull distribution [13].

In this study, ACBDV values were analyzed at 1%, 10%, and 50% breakdown risk probabilities for each sample. These values are important for identifying the risk of insulation failure over time so as to achieve the longevity of the polymeric material. To evaluate the lowest possible ACBDV of the polymeric samples, especially for the HV equipment, the 1% breakdown risk probability was used. The 10% risk probability was taken into account to establish an early warning benchmark or threshold to the expected failure, while the 50% cumulative probability risk was considered to determine the safety coefficient for the electric equipment design.

III. EXPERIMENTAL SET-UP

A. Sample Preparation

Seven types of polymeric insulation samples were prepared using 2-mil (0.05mm) Nomex paper, varnish, and NPs.

Initially, Nomex polymeric samples with a length of 17.5 cm and a width of 7.5 cm were collected and dried at 130 °C for 120 h. Then, the samples went through the NP-based varnish solution and Vacuum Pressure Impregnation (VPI) method. In this process, three types of NPs were incorporated into the vanish solution:

- Al_2O_3 (Average Particle Size (APS): 65 nm),
- TiO_2 (APS: 70 nm),
- Fe_3O_4 (APS: 50 nm),

each at concentration of 0.5wt% and 1wt%. The maximum concentration was considered to be 1wt% to ignore the agglomeration problem.

A picture of the prepared test sample is illustrated in Figure 1, and the description of these samples is provided in Table I.

Fig. 1. Photograph of the prepared test sample S1.

TABLE I. DESCRIPTION OF THE TEST SAMPLES

Sample nomenclature	Description
S1	Nomex + Varnish
S2	Nomex + Varnish + 0.5wt% Al_2O_3
S3	Nomex + Varnish + 0.5wt% TiO_2
S4	Nomex + Varnish + 0.5wt% Fe_3O_4
S5	Nomex + Varnish + 1wt% Al_2O_3
S6	Nomex + Varnish + 1wt% TiO_2
S7	Nomex + Varnish + 1wt% Fe_3O_4

B. Aging Process

According to the IEEE standards, the maximum insulation temperature of the Nomex VPI should be within the range of 130 °C – 150 °C and the average rise in the winding temperature should also be within the range of 60 °C – 80 °C [14, 15]. Taking this into account, the test samples were subjected to accelerated thermal aging at 145 °C for 600 h into a temperature-controlled shielded aging chamber. During the thermal aging process, every 100 h of instant aging, the samples were kept out of the chamber and the experimentation was performed.

C. Experimental Set-Up of ACBDV Test

For the measurement of ACBDV, an experimental setup was developed according to IEEE standards [14, 15]. A schematic of the setup is presented in Figure 2. The measuring electrodes were attached with two wooden blocks, each measuring 24 cm in length, 8 cm in width, and 4 cm in height. The test samples were positioned between these two electrodes. The lower wooden block was fitted with a metal plate, serving as the Low-Voltage (LV) electrode, while the upper block was equipped with a metal rod (diameter of 0.5 mm) utilized as the HV electrode. The experimental measurements were performed at room temperature, sixteen times for every type of the test polymeric insulation samples.

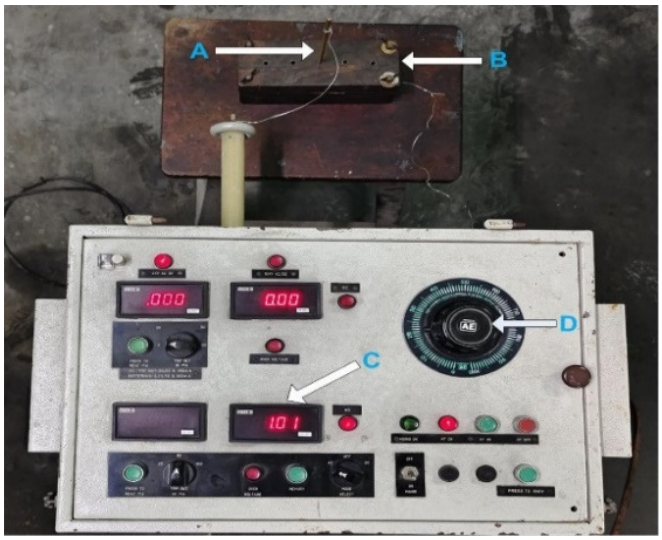

Fig. 2. Experimental set-up for the ACBDV measurement. (A) Metal rod (HV electrode), (B) Sample placed between two electrodes, (C) BDV display, and (D) Voltage regulator.

IV. RESULTS AND DISCUSSIONS

A. Fourier Transform Infrared Spectroscopy

FTIR spectroscopy was employed to examine the impact of thermal aging and NP-induced modifications on the chemical composition and functional groups of Nomex insulation. Each polymeric sample was analyzed at three aging stages: unaged, 300 h aged, and 600 h aged. Important peaks from the FTIR spectra of pristine and NC-based Nomex samples at different aging durations are displayed in Figures 3 and 4. A narrow distribution of peaks within the 1000 - 1700 cm^{-1} range was observed due to the presence of *meta*-diphenyl and amide groups in the Nomex macromolecule. The characteristic peak of Nomex insulation related to the amide II band (N-H bending and C-N stretching) was observed at 1523 cm^{-1}. Additionally, as shown in Figure 4, an absorption peak corresponding to the Al-O bond was noted near 630 cm^{-1}, confirming the incorporation of α-Al_2O_3 molecules [16].

The majority of these peaks in S5 have exhibited minimal changes with increasing aging. During thermal aging, the chemical decomposition of the polymer network in Nomex insulation was mainly driven by two processes, namely hydrolysis and pyrolysis.

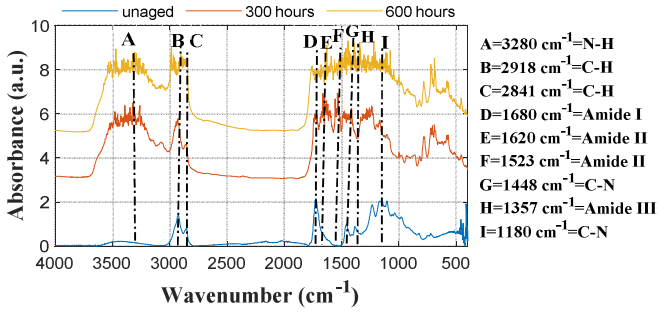

Fig. 3. ATR-FTIR spectrum of S1 at unaged and different aging durations.

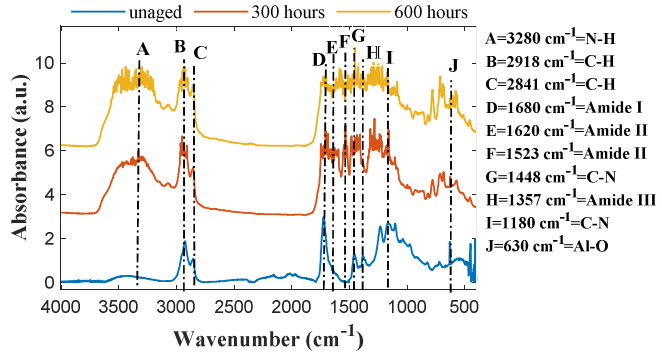

Fig. 4. ATR-FTIR spectrum of S5 at unaged and different aging durations.

The hydrolysis temperature was lower than that for pyrolysis, especially in samples with higher moisture ingress [15]. The presence of moisture enhanced the hydrolysis reaction, which destroyed the amide bond of the Nomex resulting in the formation of hydrophilic hydroxyl and amino groups. These chemical reactions were evident in the FTIR spectra of S1 and S5, particularly in regions of 3200 - 3650 cm^{-1} and 1180 cm^{-1}. The absorption peaks within 3200 - 3650 cm^{-1} corresponded to hydroxyl (-OH) groups, whose intensities increased due to hydrolysis reaction with the penetrated water in most of the Nomex polymeric samples. Further, the reduction in peaks associated with C-N stretching vibration in the amide III band of C – N - H at 1180 cm^{-1} signified a rapid degradation in the backbone structure of the Nomex. Nevertheless, the FTIR analysis revealed that the decrease in both of these peaks was substantially lower in the alumina-based NC sample (S5) compared to that of S1. Therefore, it can be suggested that the NP addition helps to restrict the thermal degradation of the Nomex polymer.

B. Average AC Breakdown Voltage

In this section, the power frequency breakdown voltage of different prepared samples (S1- S7) with various aging states was analyzed.

1) ACBDV of Different Prepared Samples

To investigate the impact of NP incorporated Nomex samples on the breakdown characteristics, the ACBDV of seven types of prepared unaged Nomex-based polymeric samples is depicted in Figure 5. It can be observed that, the nanofiller addition enhanced the ACBDV values for the samples S5 - S7. According to [4], the incorporation of NPs enabled the modulation in the interfacial stoichiometry of polymeric insulation.

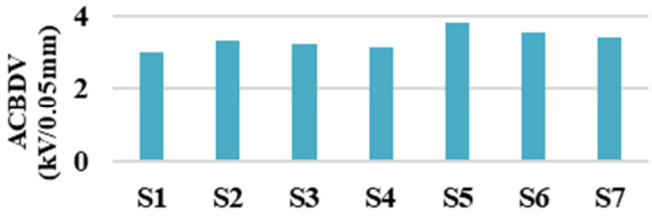

Fig. 5. The average ACBDV of prepared unaged samples.

According to the multicore model, the first and second layers at the NP/polymer interface played a critical role in the formation of deep traps within the polymer matrix [17]. These NP-induced deep traps, displayed in Figure 6, created localized energy sites that restrict the electron movement through the polymer's crystalline regions, thereby enhancing the BDV of NC polymer samples [18].

The observed improvements in ACBDV correlated well with the FTIR data (Figures 4 and 5). In the unaged samples (S5 – S7), stable hydrogen-bond peaks at 3200 – 3280 cm^{-1} indicated preserved H-bonding, which strengthened the Nomex insulation and supported the deep-trap formation [19]. Additionally, the NC samples incorporating 0.5 wt% and 1 wt% alumina NPs demonstrated the highest BDV performance. In contrast, weakened aromatic C – N peaks at 1448 cm^{-1} in S6 and S7 suggested that TiO_2 and Fe_3O_4 may have partially disrupted aramid rings. This disruption weakened the polymer's tacticity, causing the development of disordered amorphous regions inside the polymer [4]. However, in the unaged Al_2O_3 sample (S5), the C-N stretching vibrations remained stable, confirming the absence of weakening effects. As a result, TiO_2 and Fe_3O_4 based NC samples exhibited slightly lower average BDV values compared to S2 and S5.

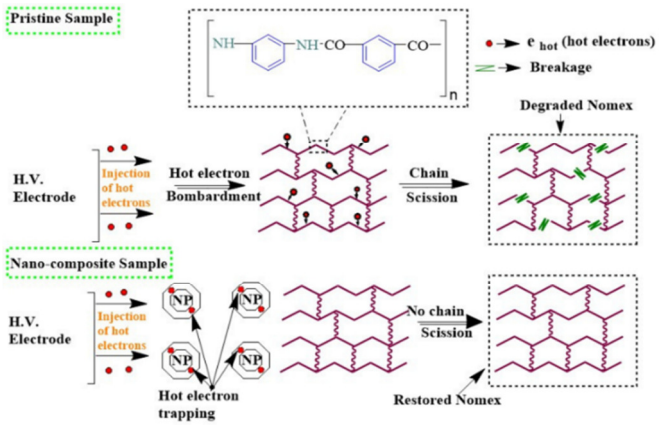

Fig. 6. Schematic presentation of charge trapping induced improvement of Nomex polymer.

2) ACBDV with Varying Aging Duration

The ACBDV of the prepared insulation samples under various aging states is presented in Figure 7. A gradual decrease in ACBDV was observed across all samples as

thermal aging increased [15]. Aging caused Nomex pulps to scatter and fibers to crack, creating loosely bound, disordered regions with poor interfacial bonding. These changes resulted in the formation of amorphous regions and shallow traps that facilitated more conductive pathways, further reducing ACBDV [16]. The FTIR analysis supported these findings, showing increasing peaks between 3200 – 3650 cm^{-1}. This indicated a rise in hydroxyl groups due to the hydrolysis from moisture ingress. Consequently, the S1 sample exhibited a sharp decline in BDV over the aging period. In contrast, the NC samples often display higher BDV than pristine Nomex. Specifically, the amide III C – N – H band at 1180 cm^{-1} showed a significant reduction in S1 after 300 – 600 h of thermal aging, while the NC samples remained relatively stable, suggesting a lower polymer degradation. This stability was possibly due to the phonon scattering mechanisms, as illustrated in Figure 8, which help preserve the Nomex structure.

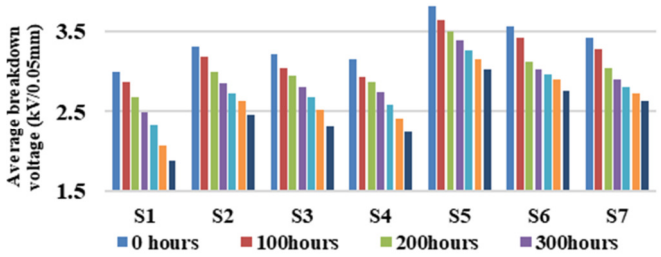

Fig. 7. ACBDV of the samples at different aging durations.

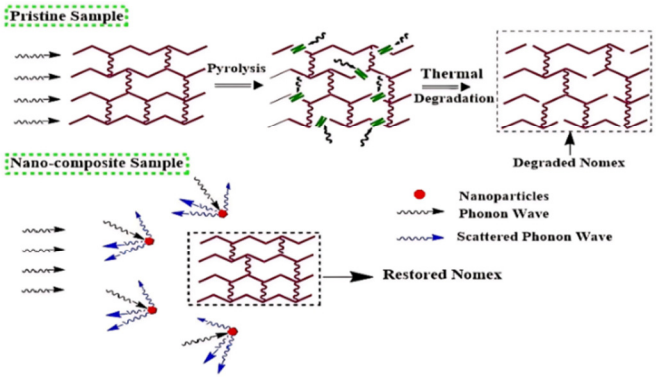

Fig. 8. Phonon scattering induced improvement of Nomex polymer.

In contrast, the TiO_2 (S6) and Fe_3O_4 (S7) NC samples exhibited a greater decline in ACBDV with aging. The FTIR analysis revealed a minimal reduction in the C – N stretching peak at 1357 cm^{-1} for S5, while S6 and S7 displayed a more pronounced decrease in this peak (1350 – 1360 cm^{-1}), indicating greater molecular degradation. This breakdown of the Nomex molecular chains promoted a transition from crystalline to amorphous regions, increasing the disorder at the NP/polymer interface. The resulting shallow traps enhanced the electron hopping and secondary electron emission, leading to a slightly accelerated breakdown process in the TiO_2 and Fe_3O_4 samples compared to Al_2O_3.

C. Statistical Analysis of AC Breakdown Voltage

For the statistical analysis of the breakdown strength for different prepared samples with various aging status, the Weibull distribution method was considered. Figures 9 and 10 illustrate the Weibull risk probability plots for the S1, S5, S6, and S7 samples with different aging years. The scale parameter (a), shape parameter (β), and p-values were calculated based on the measured ACBDV data (t).

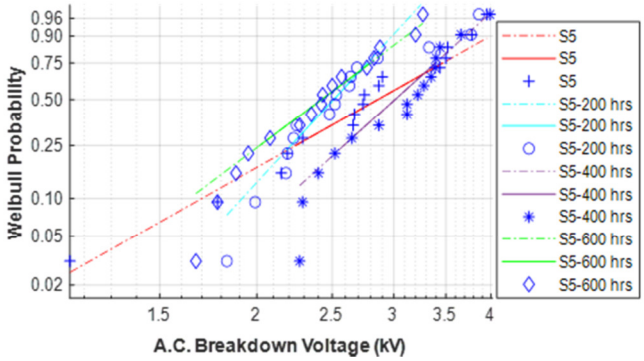

Fig. 9. Weibull distribution of ACBDV for S1.

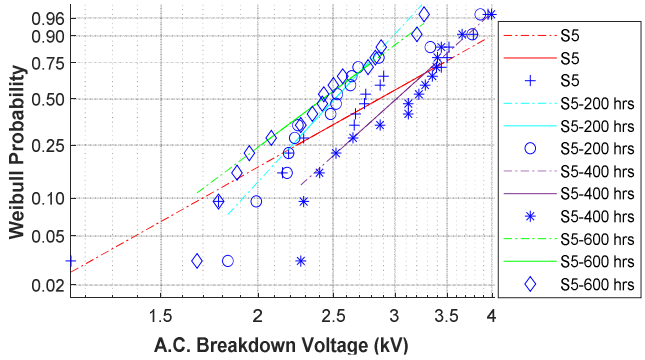

Fig. 10. Weibull distribution of ACBDV for S5.

These statistical values are summarized in Table II for all samples. It can be observed that the majority of the samples exhibited p-values greater than 0.05, indicating that the breakdown voltage dataset followed the Weibull distribution.

1) Weibull Probability for Different Prepared Samples

The ACBDV, denoted as E, at 1%, 10%, and 50% breakdown risk probabilities for the prepared insulation samples (S1 - S7) was calculated and the results are presented in Table III. The incorporation of Al_2O_3, TiO_2, and Fe_3O_4 in the Nomex polymer improved the breakdown strength across all three risk levels.

Specifically, the addition of Al_2O_3 NPs enhanced the dielectric strength of Nomex insulation by adsorbing the surface charges and introducing deep charge traps through the modulation of localized energy states [19]. The charges injected from the electrodes were captured in these deep traps and should overcome the interfacial energy barriers at the NP-polymer interface. Additionally, the strong hydrogen bonding in Al_2O_3 - based NCs also helped scatter the phonon waves,

slowing thermal degradation of the polymer backbone and reducing defect formation. Consequently, samples S2 and S5 maintained deeper trap levels compared to the unfilled S1.

TABLE II. CONFORMITY FOR WEIBULL DISTRIBUTION PLOTS AT DIFFERENT AGING DURATIONS

Sample	Aging duration (h)	α	β	*p*-value	Conformity
S1	0	2.8803	6.8595	0.1067	Accepted
	200	3.9477	3.7934	0.0916	Accepted
	400	3.1077	6.3049	0.0147	Not accepted
	600	3.3884	6.5355	0.0010	Not accepted
S2	0	2.8607	6.0563	0.2012	Accepted
	200	3.4954	6.9297	0.7421	Accepted
	400	3.4677	10.3451	0.1369	Accepted
	600	3.1160	10.4455	0.0305	Not accepted
S3	0	3.3618	10.5411	0.2599	Accepted
	200	3.1717	7.7087	0.9946	Accepted
	400	3.3732	8.3598	0.1177	Accepted
	600	3.0615	6.4128	0.0297	Not accepted
S4	0	3.192	5.2848	0.1694	Accepted
	200	3.0925	5.7208	0.7945	Accepted
	300	3.0127	5.5079	0.0920	Accepted
	400	3.2281	6.2601	0.0575	Accepted
	600	2.6499	7.2201	0.0207	Not accepted
S5	0	3.0445	4.4056	0.4661	Accepted
	200	2.8582	4.6501	0.9566	Accepted
	400	3.2696	7.129	0.1955	Accepted
	600	2.6225	5.7501	0.2575	Accepted
S6	0	2.9714	6.8207	0.0572	Accepted
	200	3.1694	7.2254	0.9608	Accepted
	400	3.3484	7.3229	0.3949	Accepted
	600	2.5913	7.4592	0.0587	Accepted
S7	0	2.7766	6.4065	0.4083	Accepted
	200	3.2126	8.9070	0.9535	Accepted
	400	3.3332	7.4627	0.2601	Accepted
	600	2.4606	7.6161	0.1461	Accepted

Additionally, semiconductive TiO_2 NPs (bandgap ~3.2 eV) generated even deeper traps due to their lower energy gap relative to the base polymer. The rutile phase of TiO_2 acted as an electron scavenger, capturing high-energy electrons and preventing their participation in conduction processes, thereby enhancing the dielectric strength [20].

Similarly, Fe_3O_4 NPs had the ability to modulate the charge conduction mechanism in a bulk polymer as an exciton killer. At a higher electric field, injected charges with opposite polarities might have participatet in the charge recombination process, as a result of which UV radiation was induced. This could initiate a chain scission reaction developing in the segmentation of long polymeric chains. However, Fe_3O_4 NPs acted as quantum dots that absorb this UV radiation, thereby mitigating the polymer degradation. This mechanism served as a beneficial factor in inhibiting the charge migration from the HV electrode to the ground electrode and suppressed the streamer formation, thus reducing the breakdown probability.

From Table III, it can also be stated that the breakdown probability for S2 and S5 was higher at 50% cumulative probability among all prepared samples. In contrast, the probability of S1 had the lowest BDV at the same probability level. Since 50% cumulative probability was associated with the mean value, the insulation with higher BDV at this probability was more suitable.

2) Weibull Probability with Several Aging Durations

ACBDV at 1%, 10%, and 50% breakdown risk probabilities of the prepared polymeric samples with different aging duration (100 h – 600 h) were calculated and were also presented in Table III.

A decline in the breakdown strength was observed with increasing aging duration, likely due to the collapse of the crosslinked 3D polymer network and increased charge migration. However, NP-modulated stoichiometry could influence the charge conduction, thus enhancing ACBDV. As dielectric degradation progressed, the surface morphology also changed. Breakdown voltages at 1% and 50% cumulative probabilities were higher in the NC samples compared to pristine Nomex, even after prolonged aging, confirming the positive impact of the NP addition. NPs enhanced the charge trapping and de-trapping at shallow traps, facilitating a faster charge carrier transfer. According to the band theory, a charge accumulation layer is formed at the electrode-polymer interface to equalize Fermi levels. In these samples, the presence of NPs introduced additional trap sites due to the increased ionized energy levels and induced dipole moments under the electric field.

Among all samples, S5 (1 wt% Al_2O_3) displayed the highest breakdown probability, while S1 (pure Nomex) showed the lowest.

TABLE III. BREAKDOWN RISK PROBABILITIES FOR DIFFERENT AGING DURATIONS

Sample	Aging duration (h)	*E* at 1%	*E* at 10%	*E* at 50%
S1	0	0.1562	2.0399	2.9518
	200	0.0780	0.9911	2.6611
	400	0.0460	0.5529	2.2979
	600	0.0385	0.3143	1.8076
S2	0	1.2103	2.3978	3.2762
	200	0.7841	1.8414	2.9423
	400	0.5298	1.2678	2.6973
	600	0.4281	0.6853	2.4072
S3	0	1.1239	2.2591	3.1774
	200	0.4764	1.7683	2.8795
	400	0.3608	1.1366	2.6192
	600	0.2652	0.5052	2.2709
S4	0	0.6141	2.1969	3.1297
	200	0.3973	1.5818	2.8002
	400	0.2401	0.9124	2.5347
	600	0.1257	0.4171	2.1745
S5	0	2.2063	2.8314	3.7843
	200	1.8062	2.1133	3.4641
	400	1.4609	1.6571	3.2056
	600	0.9922	1.1819	2.9494
S6	0	1.8661	2.6756	3.5003
	200	1.5874	2.0103	3.0778
	400	1.2721	1.4637	2.8791
	600	0.8246	0.9820	2.6915
S7	0	1.5556	2.5226	3.3764
	200	1.2103	1.9464	3.0023
	400	0.8549	1.3538	2.7627
	600	0.6684	0.8087	2.5739

V. CONCLUSIONS

This study investigated the effect of incorporating Al_2O_3, TiO_2, and Fe_3O_4 Nanoparticles (NPs) into Nomex polymer insulation on AC Breakdown Voltage (ACBDV). A detailed analysis was conducted to understand how NP-induced chemical modifications influence the suppression of ACBDV degradation over thermal aging. Nomex-based Nanocomposite (NC) samples were thermally aged at 145 °C for 600 h and their dielectric reliability was assessed using Weibull statistical analysis at 1%, 10%, and 50% risk probabilities.

The Fourier Transform Infrared Spectroscopy (FTIR) results revealed that the preservation of C–N stretching vibrations in Al_2O_3-based samples (S2, S5) correlated strongly with a superior breakdown strength. Among all NCs, the addition of NPs significantly enhanced ACBDV, with improvements of 63.16% (Al_2O_3), 48.89% (TiO_2), and 42.39% (Fe_3O_4) compared to pristine Nomex after 600 h of aging. Among all NCs, sample S5 (1 wt% Al_2O_3) consistently exhibited superior performance across all aging states and risk levels.

ACKNOWLEDGMENT

The Financial support for this work has been provided by SERB, Government of India (Grant no SERB (DST)-CRG/2022/008028.

REFERENCES

[1] M. F. Abdelkarim, L. S. Nasrat, S. M. Elkhodary, A. M. Soliman, A. M. Hassan, and S. H. Mansour, "Volume Resistivity and Mechanical Behavior of Epoxy Nanocomposite Materials," *Engineering, Technology & Applied Science Research*, vol. 5, no. 2, pp. 775–780, Apr. 2015, https://doi.org/10.48084/etasr.536.

[2] L. Madani, K. S. Belkhir, and S. Belkhiat, "Experimental study of electric and dielectric behavior of PVC composites," *Engineering, Technology & Applied Science Research*, vol. 10, no. 1, pp. 5233–5236, 2020.

[3] "Excellent Properties of Nomex® 410 Enable Long-term Reliability," DuPont, https://www.dupont.com/news/nomex-410.html.

[4] S. K. Paul, S. Maur, S. Biswas, and A. K. Pradhan, "Review on Thermal and Electrical Properties for Condition Assessment of Epoxy Nano-Composites by Advanced Techniques," *IEEE Transactions on Dielectrics and Electrical Insulation*, vol. 31, no. 1, pp. 230–245, Feb. 2024, https://doi.org/10.1109/TDEI.2023.3313995.

[5] S. Maur, B. Chakraborty, A. K. Pradhan, S. Dalai, and B. Chatterjee, "A Novel Approach to Estimate Electrothermal Aging of Epoxy–Alumina Nanocomposites Using Dielectric Relaxation Current Analysis," *IEEE Transactions on Dielectrics and Electrical Insulation*, vol. 30, no. 1, pp. 41–48, Feb. 2023, https://doi.org/10.1109/TDEI.2022.3227885.

[6] Y. Hou, Z. Zhang, J. Zhang, Z. Wang, and H. Liu, "Experimental investigations into the enhanced dielectric breakdown performances of propylene carbonate modified by TiO2 nano-particles," *IEEE Transactions on Dielectrics and Electrical Insulation*, vol. 23, no. 5, pp. 2816–2821, Oct. 2016, https://doi.org/10.1109/TDEI.2016.7736841.

[7] Y. Wei, B. Han, X. Hu, Y. Lin, X. Wang, and X. Deng, "Synthesis of Fe3O4 Nanoparticles and their Magnetic Properties," *Procedia Engineering*, vol. 27, pp. 632–637, Jan. 2012, https://doi.org/10.1016/j.proeng.2011.12.498.

[8] T. Kiyan, T. Ihara, S. Kameda, T. Furusato, M. Hara, and H. Akiyama, "Weibull Statistical Analysis of Pulsed Breakdown Voltages in High-Pressure Carbon Dioxide Including Supercritical Phase," *IEEE Transactions on Plasma Science*, vol. 39, no. 8, pp. 1729–1735, Aug. 2011, https://doi.org/10.1109/TPS.2011.2159135.

[9] G. D. Peppas, V. P. Charalampakos, E. C. Pyrgioti, M. G. Danikas, A. Bakandritsos, and I. F. Gonos, "Statistical investigation of AC breakdown voltage of nanofluids compared with mineral and natural ester oil," *IET Science, Measurement & Technology*, vol. 10, no. 6, pp. 644–652, Sep. 2016, https://doi.org/10.1049/iet-smt.2016.0031.

[10] T. W. Anderson and D. A. Darling, "Asymptotic Theory of Certain 'Goodness of Fit' Criteria Based on Stochastic Processes," *The Annals of Mathematical Statistics*, vol. 23, no. 2, pp. 193–212, Jun. 1952.

[11] U. Khaled and A. Beroual, "AC dielectric strength of synthetic ester-based Fe3O4, Al2O3 and SiO2 nanofluids — conformity with normal and weibull distributions," *IEEE Transactions on Dielectrics and Electrical Insulation*, vol. 26, no. 2, pp. 625–633, Apr. 2019, https://doi.org/10.1109/TDEI.2018.007759.

[12] S. S. Shapiro and M. B. Wilk, "An analysis of variance test for normality (complete samples)," *Biometrika*, vol. 52, no. 3–4, pp. 591–611, Dec. 1965, https://doi.org/10.1093/biomet/52.3-4.591.

[13] M. P. Wilson *et al.*, "Impulse-driven Surface Breakdown Data: A Weibull Statistical Analysis," *IEEE Transactions on Plasma Science*, vol. 40, no. 10, pp. 2449–2456, Oct. 2012, https://doi.org/10.1109/TPS.2011.2181172.

[14] *IEEE Standard Test Code for Dry-Type Distribution and Power Transformers*, C57.12.91, 2001.

[15] *IEEE Standard Test Procedure for Thermal Evaluation of Insulation Systems for Ventilated Dry-Type Power and Distribution Transformers*, C57.12.56, 1986.

[16] L. Li *et al.*, "Effects of ambient humidity and thermal aging on properties of Nomex insulation in mining dry-type transformer," *High Voltage*, vol. 6, no. 1, pp. 71–81, 2021, https://doi.org/10.1049/hve.2019.0293.

[17] T. Tanaka, M. Kozako, N. Fuse, and Y. Ohki, "Proposal of a multi-core model for polymer nanocomposite dielectrics," *IEEE Transactions on Dielectrics and Electrical Insulation*, vol. 12, no. 4, pp. 669–681, Aug. 2005, https://doi.org/10.1109/TDEI.2005.1511092.

[18] B. Du, P. Huang, and Y. Xing, "Surface charge and flashover characteristics of fluorinated PP under pulse voltage," *IET Science, Measurement & Technology*, vol. 11, no. 1, pp. 18–24, 2017, https://doi.org/10.1049/iet-smt.2016.0103.

[19] Y. Zhang *et al.*, "Space Charge Characteristics at the Interface of Laminated Epoxy Resin," *Molecules*, vol. 28, no. 14, Jul. 2023, Art. no. 5537, https://doi.org/10.3390/molecules28145537.

[20] C. Liu, K. Shih, Y. Gao, F. Li, and L. Wei, "Dechlorinating transformation of propachlor through nucleophilic substitution by dithionite on the surface of alumina," *Journal of Soils and Sediments*, vol. 12, no. 5, pp. 724–733, May 2012, https://doi.org/10.1007/s11368-012-0506-0.